

Extra-galactic magnetic fields and the second knee in the cosmic-ray spectrum

Martin Lemoine

Institut d'Astrophysique de Paris, CNRS, 98 bis Boulevard Arago, F-75014 Paris, France

(dated: October 31, 2019)

Recent work suggests that the cosmic ray spectrum may be dominated by Galactic sources up to $10^{17.5}$ eV, and by an extra-Galactic component beyond, provided this latter cut-off below the transition energy. Here it is shown that this cut-off could be interpreted as a signature of extra-galactic magnetic fields with equivalent average strength B and coherence length l_c such that $B^2 l_c^2 \approx 2 \cdot 10^{10} \text{ G Mpc}^2$, assuming $l_c < r_L$ (Larmor radius at $< 10^{17}$ eV) and continuously emitting sources with density 10^{-5} Mpc^{-3} . The extra-Galactic flux is suppressed below 10^{17} eV as the diffusive propagation time from the source to the detector becomes larger than the age of the Universe.

PACS numbers: 98.70.Sa, 98.65.Dx

Introduction. Recent developments, both experimental and theoretical, have significantly broadened the landscape of ultra-high energy cosmic ray phenomenology. The High Resolution Fly's Eye experiment has reported the detection of a high energy cut-off at 10^{20} eV [1], as would be expected from a cosmological population of sources. This experiment has also found that the chemical composition is dominated by protons down to 10^{18} eV, and by heavy nuclei further below, in agreement with preliminary KASCADE data [2]. This and the steepening of the cosmic-ray spectrum at the "second knee" at $10^{17.5}$ eV suggest the disappearance of the low-energy (heavy nuclei) component and the nearly simultaneous emergence of a high-energy (proton) component. On theoretical grounds, it has been observed by Berezhinsky et al. [3] that a cosmological distribution of sources producing a single powerlaw could cut the high energy part of the cosmic-ray spectrum from the second knee up to the cut-off at 10^{20} eV, including the dip of the "ankle" at $10^{18.5}$ eV. In light of these results, it is thus tempting to think that the cosmic-ray spectrum consists of only two main components: one Galactic, another extra-galactic, with the transition around the second knee [4].

However this model requires to impose a low-energy cut-off on the extra-galactic spectrum around 10^{18} eV in order to not overproduce the flux close to the second knee; and the exact position of this cut-off as well as the spectral slope below it must be tuned to how the Galactic component extends above the knee [5].

The objective of the present work is to demonstrate that this cut-off could be interpreted as a signature of extra-galactic magnetic fields with average strength B and coherence length l_c such that $B^2 l_c^2 \approx 2 \cdot 10^{10} \text{ G Mpc}^2$, assuming $l_c < r_L$ (Larmor radius at $< 10^{17}$ eV) and continuously emitting sources with density 10^{-5} Mpc^{-3} . In this picture, the extra-Galactic spectrum shuts off below 10^{17} eV as the diffusion time to the closest sources becomes larger than the age of the Universe. The first knee is viewed here as the maximal injection energy for protons at the (Galactic) source.

The existence of extra-galactic magnetic fields is of importance to various fields of astrophysics, including ultra-

high energy cosmic ray phenomenology, but very little is known on their origin, on their spatial configuration and on their amplitude [6]. The best upper limits on $B^2 l_c^2$ from Faraday observations lie some two orders of magnitude above the value suggested here. In the present framework, experiments such as KASCADE-Grande [2] could probe these magnetic fields thanks to accurate measurements of the spectrum and composition in the range $10^{16} - 10^{18}$ eV.

Particle propagation. The main effect of extra-galactic magnetic fields on 10^{17} eV particles is as follows. In a Hubble time, these particles travel by diffusing on magnetic inhomogeneities a distance $\approx \chi_0^{-1} l_{\text{scatt}}^{1=2}$, 65 Mpc ($l_{\text{scatt}}=1 \text{ Mpc}$)¹⁼², with l_{scatt} the scattering length of the particle. If χ_0 is much smaller than the typical source distance, the particle cannot reach the detector in a Hubble time; since l_{scatt} , hence χ_0 , increases with increasing energy, this produces a low-energy cut-off in the propagated spectrum. Current data at the highest energies, notably the clustering seen by various experiments, suggests a cosmic-ray source density $n \approx 10^{-6} - 10^{-5} \text{ Mpc}^{-3}$ [7], which corresponds to a source distance scale $\approx 50 - 100 \text{ Mpc}$. Hence $l_{\text{scatt}} < 0.3 - 1 \text{ Mpc}$ at 10^{17} eV would shut off the spectrum below this energy [8].

To become more quantitative one has to calculate the propagated spectrum and compare it to the observed data. The low energy part ($< 10^{18}$ eV in what follows) of the extra-galactic proton spectrum diffuses in the extra-galactic magnetic field since the diffusion path length l_{diff} , where $l_{\text{loss}} \approx 1 \text{ Gpc}$ (at 10^{18} eV) is the energy loss length. In contrast, particles of higher energies ($> 4 \cdot 10^{18}$ eV in what follows) travel rectilinearly since $l_{\text{diff}} > l_{\text{loss}}$. In the diffusion approximation, the propagated differential spectrum reads [9]:

$$J_{\text{di}}(E) = \frac{c}{4} \sum_i^Z \int dt \int_X \frac{e^{-r_i^2/(4t^2)}}{(4t^2)^{3=2}} \frac{dE_g(t;E)}{dE} Q(E_g(t;E)) \quad (1)$$

The sum carries over the discrete source distribution. The function $Q(E_g) = K(E_g/E_{\text{max}})$ gives the emission

rate per source at energy E_g , K a normalization factor such that $dE E Q(E) = L$, with L the total luminosity, which is assumed to scale as the cosmic star formation rate from [10]. However a similar fit could be obtained by modifying by 0.1 for a different scaling [3], hence this hypothesis is not crucial to the present analysis. The injection spectrum extends from a minimum energy ($< 10^{16}$ eV in the present model) up to $E_{max} = 10^{22}$ eV (the exact value is of little importance here). The function $E_g(t; E)$ defines the energy of the particle at time t , assuming it has energy E at time t_0 . This function and its derivative dE_g/dE can be reconstructed by integrating the energy losses [3].

Accounting for energy losses, the path length is defined as:

$$l(t; E) = \frac{c}{3} \int_{t_0}^t \frac{dt}{a(t)} l_{scatt} [E_g(t; E)]^{1=2}; \quad (2)$$

where the scale factor $a(t)$ (normalized to unity today) appears in defining a comoving path length (with l_{scatt} the comoving scattering length) [11]. The dynamics of the scale factor is of little importance here. In fact the Syrovatsky solution of Eq. (1) is only valid for time-independent energy losses in a non-expanding space-time. However it remains a good approximation to the actual solution at the low energies of interest since the energy loss time H_0^{-1} below 10^{19} eV, as the expansion timescale H_0^{-1} , are much larger than the time $l_{scatt} = c$ needed to reach diffusion. Hence expansion and energy losses play a minor role in determining the shape of the spectrum in the diffusive part. Only continuously emitting sources are considered here, and the cosmological evolution of the magnetic field has been neglected for simplicity.

The time integral in Eq. (1) is bounded by the maximum lookback time t at which $E_g(t; E) = E_{max}$ and by the minimum lookback time t_0 $t_0 = t - l_{scatt} = c$ necessary to enter the diffusing regime, taken to be the solution of $r(t) = l(t; E)$, where $r(t) = \int_{t_0}^t dt' a(t')$ is the comoving light cone distance.

At higher energies, the propagated spectrum is given by:

$$J_{rect}(E) = \frac{1}{4} \sum_i X \frac{1}{4 r_i^2} \frac{dE_g(t_i; E)}{dE} Q [E_g(t_i; E)]; \quad (3)$$

and t_i in Eq. (3) is related to r_i by $r_i = \int_{t_i}^{R_{t_0}} dt' a(t')$; r_i should not exceed $l(t_i; E)$, beyond which point motion must have become diffusive.

The Galactic cosmic ray component is modeled as follows. Supernovae are accepted as standard acceleration sites, yet it is notoriously difficult to explain acceleration up to a maximum energy 10^8 eV. Thus it is assumed that the knee sets the maximum acceleration energy for Galactic cosmic rays: in this conservative model, the spectrum of species i with charge Z takes the form $j_Z(E) = (E = E_Z)^{-1} \exp(-E = E_Z)$, with $\alpha = 2.4 - 2.7$ a

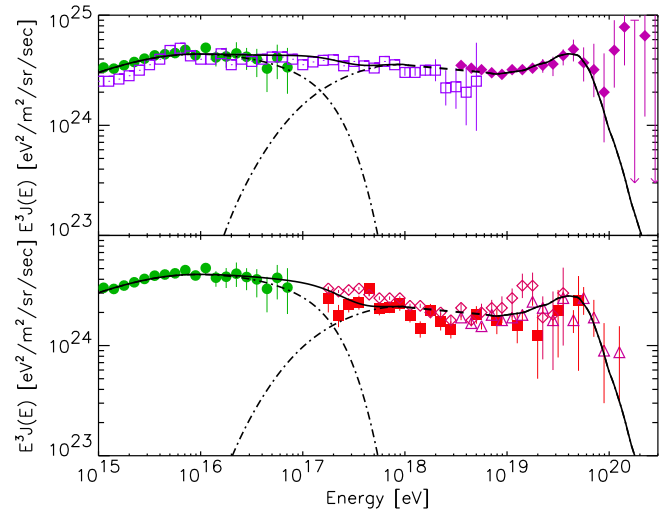


FIG. 1: Open squares: Akeno; filled circles: KASCADE; filled diamonds: AGASA; filled squares: Hires-2; open triangles: Hires-1; open diamonds: Fly's Eye. Fit of the Galactic (low-energy dot-dash line) and extra-galactic (high-energy dot-dash) to cosmic ray data. Total flux: solid line.

species dependent spectral index, $E_Z = Z E_p$ the location of the knee, with $E_p = 2 - 10$ eV [2]. This scenario is consistent with preliminary KASCADE data.

Datasets from the most recent experiments are considered here: KASCADE $10^{15} - 10^{17}$ eV [2], Akeno $10^{15} - 10^{18.6}$ eV [12], AGASA $10^{18.5} - 10^{20.5}$ eV [13], Hires $10^{17.3} - 10^{20}$ eV [1] and Fly's Eye $10^{17.3} - 10^{20}$ eV [14]. Akeno is not recent but it is the only experiment whose data bridge the gap between the knee and the ankle. These experiments use different techniques and their results span different energy ranges, hence the data do not always match. A clear example is the discrepancy between Hires and AGASA at the highest energies. In the following, the high energy datasets have been split in two groups: one with Hires and Fly's Eye, the other with Akeno and AGASA. The flux of the extra-galactic component was given two possible normalization values in order to accommodate either of these datasets, while the flux of the low energy part is scaled to the recent KASCADE data. This method is obviously less advantageous to a fit than when datasets are shifted one to one another. A more robust comparison of this model with the data will be possible with the upcoming results of the KASCADE-Grande experiment covering the range $10^{16} - 10^{18}$ eV [2].

Results. Figure 1 shows the total spectrum (Galactic + Extra-galactic) compared to the data, assuming continuously emitting sources with density $n = 10^{-5} \text{ Mpc}^{-3}$ and spectral index $\alpha = 2.6$. Locations for the first hundred closest sources (i.e. within $r = 140 \text{ Mpc}$) were drawn at random, using a uniform probability law per unit volume. For farther sources, the continuous source approximation becomes valid and it is used numerically.

Considering the difficulty of comparing different

datasets, the fit shown in Fig.1 appears overall satisfying. One should also note that this fit uses a minimum number of free parameters (λ and l_{scatt} at 10^{17} eV), in order to consider the most economical scenario. As discussed below, there are various ways in which one could extend the present analysis, although this comes at the price of handling a larger number of (unknown) parameters.

In Fig. 1, a straight dashed line was drawn across the region $10^{18} \text{--} 6 \cdot 10^6$ eV in which the propagation is neither rectilinear nor diffusive. These limits were found by comparing the diffusive and rectilinear spectra with the non-magnetic field spectrum. In this energy range the diffusive path length becomes of the same order as the rectilinear distance at some point during the particle history. The diffusion theorem [9] suggests that the flux in this intermediate region should follow the non-magnetic field spectrum (in which case it would dip $\sim 10\%$ below the dashed line around $3 \cdot 10^6$ eV). This theorem rests on the observation that integrating Eq. (1) for a continuous distribution of sources over an infinite volume gives the rectilinear spectrum Eq. (3). However the actual volume is bounded by the past light cone; this makes the diffusive spectrum shut off exponentially at energies $> 10^{18}$ eV. The rectilinear part also shuts off at energies $< 5 \cdot 10^6$ eV as the maximum lookback time that bounds the integral of Eq. (3) decreases sharply. Hence one might expect a small dip in the spectrum around $2 \text{--} 3 \cdot 10^6$ eV. Interestingly the data is not inconsistent with such a dip at that location. Monte Carlo simulations of particle propagation are best suited (and should be performed) to probe the spectrum in this region.

The scattering length was assumed to scale as $l_{\text{scatt}} \propto E^{-2}$, and its value at 10^{18} eV is 25 Mpc. This scaling of the scattering length is typical for particles with Larmor radius larger than the coherence scale of the field, in which case $l_{\text{scatt}} \sim l_c (r_L = l_c)^2$. Since the Larmor radius $r_L \sim 1 \text{ Mpc}$ ($E = 10^{18}$ eV) ($B = 10^{-9}$ G) $^{-1}$, one may expect this approximation to be valid. In effect, 1 Mpc is a strict upper bound to the coherence length of a turbulent inter-galactic magnetic field [9, 15], and available numerical simulations indicate much smaller coherence lengths [16] in clusters of galaxies. A value $l_c \sim 10$ kpc could also be expected if the inter-galactic magnetic field is produced by galactic outflows. The above condition for l_{scatt} corresponds to $B \cdot l_c \sim 2 \cdot 10^0 \text{ G Mpc}^2$ for an all-pervading magnetic field. Hence, for $l_c \sim 30$ kpc, and $B \sim 10^{-9}$ G (in order to obtain the correct scattering length at 10^{18} eV), one finds $\lambda > l_c$ for $E > 10^{16.5}$ eV.

It is possible that the scaling of l_{scatt} with energy changes in the range $10^{16} \text{--} 10^{17}$ eV as r_L may become smaller than l_c . There is no universal scaling for l_{scatt} when $r_L < l_c$ as the exact relationship then depends on the structure of the magnetic field; for instance, in Kolmogorov turbulence, one finds $l_{\text{scatt}} \propto r_L$ for $0.1 l_c < r_L < l_c$ and $l_{\text{scatt}} \propto r_L^{1/3}$ at lower energies [17]. The possible existence of regular components of extra-galactic magnetic fields may also modify l_{scatt} .

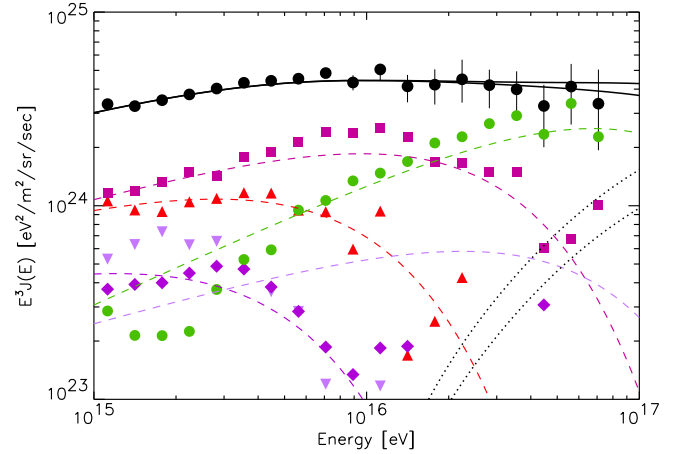


FIG. 2: KASCADE (SYBILL) data: solid lines: all-particle spectra (Galactic + extra-galactic); dotted lines: extra-galactic component; dashed lines: Galactic spectra, for p, He, C, Si and Fe, in order of increasing x axis intercept. Filled circles: all-particle; diamonds: p; upward-pointing triangles: He; squares: C; downward pointing triangles: Si; circles: Fe. Error bars on reconstructed chemical composition have been omitted for clarity, but are significant, see [2].

A change in the scaling of l_{scatt} with E , if it occurs at $E > 10^{16.5}$ eV, would imply a different value for $B \cdot l_c$, with the difference being a factor of order unity to a few. It is exciting to note that, in the present framework, experiments such as KASCADE-Grande [2] may allow to constrain the energy dependence of the scattering length (hence the magnetic field structure) by measuring accurately the energy spectrum and composition between the first and second knees.

The predictions (for both normalizations in Fig. 1) for the extra-galactic proton flux is shown and compared to the chemical composition measurement of KASCADE in Fig. 2. These composition measurements remain uncertain, as can be seen by comparing the QGSJet and SYBILL reconstructions in [2]; the proton and helium knee positions seem robust however. The dotted line represents the expected proton signal from the extra-galactic component, whose detection seems within the reach of KASCADE-Grande. One may note that Galactic spectra with exponential suppression beyond the knee agree with the KASCADE data. Nonetheless, if the Galactic spectra are found to extend as powerlaws beyond the knee, the scattering length of extra-galactic protons should be smaller by a factor of order unity (and $B \cdot l_c$ correspondingly higher).

The result for $B \cdot l_c$ depends weakly on the source density: since the cut-off energy depends on the ratio of the source distance to the path length $n^{1/3} \frac{D}{l_c} / n^{1/3} (B \cdot l_c)$, $B \cdot l_c$ scales with n according to: $B \cdot l_c \sim 2 \cdot 10^{10} (n = 10^{-5} \text{ Mpc}^{-3})^{1/3} \text{ G Mpc}^2$. Cosmic variance related to the distance D to the closest sources is significant for the low energy part $E < 10^{17}$ eV of the

spectrum. Again, since the spectrum cuts off as $\exp(-D^2/4\tau)$, the cosmic variance on D implies an uncertainty $\Delta B/B \approx \Delta D/D \approx 0.1$. The (typical) case shown in Fig. 1 corresponds to closest sources at $35 \text{ Mpc} < r < 10^3$.

The present scenario indicates that charged particle astronomy will be possible at the highest energies $> 4 \times 10^8 \text{ eV}$, since one expects deflection angles $\theta_{ms} \approx 0.5^\circ (E=10^{20} \text{ eV})^{-1} (D=100 \text{ Mpc})^{1/2} (B/B_e)^{1/2} (L_e/2 \times 10^{10} \text{ G Mpc}^2)^{1/2}$. Recent studies have attempted to obtain definite predictions for θ_{ms} by using MHD simulations of large-scale structure formation with magnetic fields scaled to reproduce existing data in clusters of galaxies [16, 18]. Their results differ widely, thereby illustrating the difficulty of constraining a priori the strength of extra-galactic magnetic fields. The present value for θ_{ms} is comparable or slightly larger than that of Ref. [16], and substantially smaller than that of Ref. [18]. The magnitude of θ_{ms} indicates that extra-galactic magnetic fields could be probed through the angular images of ultra-high energy cosmic ray point sources, and this will constitute a strong test of the present scenario.

The proposed scattering length cannot result from scattering on magnetic fields associated with galaxies or groups and clusters of galaxies, since the collision mean free path with either of these objects is too large, being $\approx 0.1 \text{ Gpc}$. The inferred magnetic field might in principle be concentrated around the source (on distance scale L) and negligible everywhere else. Since the spectrum would cut off below an energy such that $2 \times 2 \times 10^{10} \text{ kpc} > L$, this requires $B > 1 \text{ G} (L_e=10 \text{ kpc})^{1/2} (L=100 \text{ kpc})^{-1}$. This possibility cannot be excluded but it gives a non-trivial constraint on the source environment. Searches for

counterparts at the highest energies would help test this possibility: for instance, magnetic fields such as above are found in clusters of galaxies but there is no report of clusters in the arrival directions of the highest energy events. If this magnetic field is intrinsic to the source, or if the cut-off at $< 10^{18} \text{ eV}$ is due to injection physics in the source [5], then, under the present assumptions, the present work still gives a stringent upper bound on all-pervading magnetic fields. To remain conservative, one may require that the cut-off should not occur above 10^8 eV , in which case one finds $B/B_e < 10^{-9} \text{ G Mpc}^2$. This limit is still an order of magnitude below existing Faraday bounds.

The magnetic field in question thus appears intergalactic in nature, in which case it is likely to be inhomogeneously distributed on small scales. Further studies are then required to relate the average B/B_e with the actual structure and distribution of these magnetic fields. One needs to account for the possible existence of a regular magnetic field component aligned with filaments and walls, which would inhibit perpendicular transport, and consider the respective filling fractions and amplitudes of the turbulent and regular components. It would be certainly worthwhile to extend the simulations of particle propagation made in realistic magnetic fields [6, 18] to the energies of interest.

Finally there are various ways in which the present study could be extended. One should notably consider the possible energy dependences of the scattering length (including the above effects of inhomogeneous and regular magnetic fields), the role of intermittent sources, the possible cosmological evolution of the magnetic field and of the source density, among others.

-
- [1] R. U. Abbasiet al. (HiRes collaboration), PRL 92 (2004) 151101.
- [2] K. H. Kampert et al. (KASCADE collaboration), arXiv:astro-ph/0405608.
- [3] V. Berezhinsky, A. Gazizov, S. Grigorieva, arXiv:hep-ph/0204357; arXiv:astro-ph/0210095
- [4] For an alternative view, T. Wibig, A. Wolfendale, arXiv:astro-ph/0410624.
- [5] V. S. Berezhinsky, S. I. Grigorieva, B. I. Hnatyk, Astropart.Phys.21 (2004) 617.
- [6] L. M. Widrow, RevModPhys.74 (2003) 775 and references therein.
- [7] P. Blasi, D. de Marco, Astropart.Phys. 20 (2004) 559; H. Yoshiguchi, S. Nagataki, S. Tsubaki, K. Sato, Astrophys.J. 586 (2003) 1211; M. Kachelriess, D. Semikoz, arXiv:astro-ph/0405258.
- [8] Similar magnetic horizon effects have been noted in C. Isola, M. Lemoine, G. Sigl, G., 2001, PRD 65 (2002) 023004; T. Stanev, arXiv:astro-ph/0303123 (2003); O. Deligny, A. Letessier-Selvon, E. Parizot, Astropart.Phys.21 (2004) 609; T. Wibig, A. Wolfendale, arXiv:astro-ph/0406511 (2004).
- [9] R. Aloisio, V. S. Berezhinsky, arXiv:astro-ph/0403095.
- [10] V. Springel, L. Hernquist, Month.Not.Roy.Astron.Soc. 339 (2003) 312.
- [11] It is assumed $\mu = 0.3$, $\beta = 0.7$, $H_0 = 70 \text{ km/s/Mpc}$.
- [12] M. Nagano et al. (Akeno collaboration), J.Phys.G18 (1992) 423.
- [13] M. Takeda et al. (AGASA collaboration), PRL 81 (1998) 1163.
- [14] D. J. Bird et al. (Fly's Eye collaboration), Astrophys.J.424 (1994) 491.
- [15] E. Waxman, J. N. Bahcall, PRD 59 (1999) 023002.
- [16] K. Dolag, D. Grasso, V. Springel, I. Tkachev, JETP Lett.79 (2004) 583 [Pisma Zh.Eksp.Theor.Fiz.79 (2004) 719]; arXiv:astro-ph/0410419.
- [17] F. Casse, M. Lemoine, G. Pelletier, PRD 65 (2002) 023002; J. Candia, E. Roulet, JCAP 0410 (2004) 007.
- [18] G. Sigl, F. Miniati, T. A. Ensslin, PRD 68 (2003) 043002; arXiv:astro-ph/0309695; PRD 70 (2004) 043007.